ORIGINAL Aichi Gakuin Dent Sci 35 : 13–21, 2022

EVALUATION OF METAL ARTIFACTS GENERATED BY TITANIUM DENTAL IMPLANTS USING MULTI-DETECTOR COMPUTED TOMOGRAPHY

SHOKO TAKADA[1)]*, MUNETAKA NAITOH[1)]*, SHIN MIYAMAE[2)] AND EIICHIRO ARIJI [1)]

[1)] *Department of Oral and Maxillofacial Radiology, School of Dentistry, Aichi Gakuin University, Nagoya 464-8651, Japan*

[2)] *Department of Gerodontology and Home Care Dentistry, School of Dentistry, Aichi Gakuin University, Nagoya 464-8651, Japan*

SYNOPSIS

It is important for the bone condition surrounding dental implants to be accurately diagnosed by postoperative imaging during dental implant treatment.

Therefore, in the present study, CT values in regions both surrounding implants and far from them were measured using mandibular phantoms to assess the effect of metal artifact reduction in multi-detector CT.

Mandibular phantoms made using bone blocks and radiopaque acrylic resin were used. Either one or three titanium dental implants were implanted into the bone blocks. Iterative reconstruction was applied in multi-detector CT, and then single-energy metal artifact reduction (SEMAR) algorithms were applied.

Changing rates of CT values on all sides with one dental implant and on the buccal and lingual sides with three dental implants using a soft tissue reconstruction function with SEMAR were larger than those using a soft tissue image reconstruction function without SEMAR. Metal artifact indexes on the lingual side with three dental implants in images using a soft tissue reconstruction function with SEMAR were smaller than those using a soft tissue reconstruction function without SEMAR in 120-kV images.

In the present study, no effect of metal artifact reduction using the SEMAR algorithm was observed surrounding dental implants. In regions far from them, the effect of metal artifact reduction using the SEMAR algorithm was limited.

Key words: metal artifacts, dental implants, multi-detector computed tomography

INTRODUCTION

Dental implant treatment is a common prosthodontic procedures, and pure titanium (Ti) is widely used as an implant material[1)]. It is important for the bone condition surrounding dental implants to be accurately diagnosed during imaging following implant treatment, especially for the diagnosis of peri-implantitis[2-4)].

Bone changes on the mesial and distal sides of dental implants can be two-dimensionally observed using intraoral and panoramic radiography, although bucco-lingual structures overlap. However, bone changes on the buccal and lingual sides of dental implants cannot be depicted in intraoral and panoramic radiography. CT is essential for the three-dimensional diagnosis of structures surrounding dental implants. However, it is well-known that metal artifacts generated by Ti dental implants can be observed in CT.

Presently, multi-detector and cone beam CT can be applied in dental implant treatment[5-7)]. Recently, various improvements of X-ray exposure mechanics and image reconstruction methods have been made to multi-detector CT[8-14)]. Iterative reconstruction provides for

*These two authors contributed equally to this work.

Corresponding author at: Shoko Takada, Department of Oral and Maxillofacial Radiology, School of Dentistry, Aichi Gakuin University

Received for publication August 30, 2022
Accepted for publication October 19, 2022

much better image quality than conventional filtered back-projection. Metal artifact reduction algorithms are applied in addition to iterative reconstruction algorithms by some manufacturers. Metal artifact reduction using the single-energy metal artifact reduction (SEMAR) algorithm was reported in the oral cavity[9,13]. Also, dual-energy CT was reported to experimentally and clinically reduce metal artifacts in the oral cavity[8,12,14]. In many previous studies, metal artifacts generated by dental alloys were assessed using qualitative image analysis by readers and quantitative image analysis in regions far from dental alloys.

In the present study, metal artifacts generated by Ti dental implants were experimentally assessed using mandibular phantoms. CT values, for both areas surrounding dental implants and regions far from them, were measured to assess the effect of metal artifact reduction using iterative reconstruction and the SEMAR algorithm.

Materials and Methods

Objects

Four bone blocks were made from cancellous bone-equivalent material (Tough Bone Phantom, BE-N, Kyoto Kagaku, Japan). The size of each bone block was 31 mm in mesio-distal length, 20 mm in height, and 10 mm in width. Into two of the four bone blocks, one dental implant and three implants were placed, respectively. The size of each dental implant (Certain PREVAIL, BIONET 3i Japan, Tokyo, Japan) was 10 mm in length and 4 mm in diameter. Additionally, three holes with a 2-mm diameter were formed in the other two bone blocks. The positions of the implants or holes, which simulated the posterior region from the second premolar to second molar, are shown in Fig. 1. Bone blocks with one or three dental implants were located in the right posterior region of an acrylic vessel (diameter: 15 cm), and one of the two bone blocks with three holes was set in the left posterior region. The one remaining bone block with three holes was used as a control. Radiopaque acrylic resin was used in the anterior and mandibular ramus regions (Fig. 2). The acrylic vessel was filled with water to simulate the soft tissue volume.

Multi-detector computed tomography

A multi-detector CT unit (Aquilion PRIME, Canon Medical Systems, Tochigi, Japan) was used. Tube voltages were set at 120- and 135-kV, and tube currents were set at 100 and 70 mA, respectively. Radiation doses with a volume CT dose index (CTDIvol) were almost the same in 120- and 135-kV CT. An adaptive iterative dose reduction three-dimensional (AIDR 3D) algorithm (degree: weak) was applied. Two-image reconstruction functions were used for soft tissue and bone images, and additionally, the SEMAR algorithm was applied in a soft tissue reconstruction function. The images were

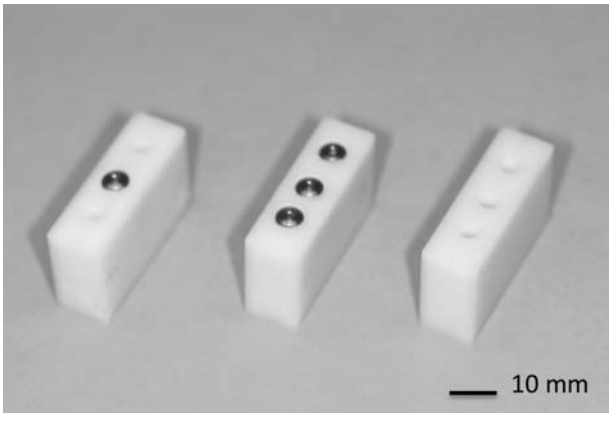

Fig. 1. Bone blocks with implants and holes

Fig. 2. Mandibular phantom made using the bone blocks and radiopaque acrylic resin

A bone block with titanium dental implant was set on the right side of an acrylic vessel, and a bone block with holes was set on the left side.

reconstructed with 1-mm-thick slices at 0.5-mm intervals. CT was repeated three times in the same way.

Multi-detector CT images

An axial image with one or three dental implants in the mid supero-inferior dental implant was displayed on a computer, and average images with a 3-mm thickness were reconstructed using 3-D visualization and measurement software (OsiriX Imaging Software, Geneva, Switzerland) in each reconstructed condition. In a control, the average images with a 3-mm thickness were reconstructed in the same way. CT values (Hounsfield Units, HU) surrounding the implants, and in regions far from them were measured.

Measurements of CT values surrounding dental implants

Rectangular regions of interests (ROIs) were set on the buccal, lingual, mesial, and distal sides of dental implants in the first molar region using average images (Fig. 3). The size of ROIs was 4 mm in length and 1 mm in width. Measurements of CT values were repeated five times in each region, and they were averaged. Also, measurements of control CT values were performed in the same way. Then, changing rates were calculated using the following formula:

Changing rate (%) = |mean CT values with one or three dental implants - mean control CT values| x 100 / mean control CT values.

Measurements of CT values in regions far from dental implants

CT values in regions far from dental implants were measured using average images with one or three dental implants and in a control. ROIs were set at 10, 20, and 30 mm on the buccal and lingual sides from the center of the bone block, and they were located in a water portion. Moreover, ROIs were set at 20 mm on the mesial and distal sides of the dental implant in the first molar region, and they were located in a radiopaque acrylic resin portion (Fig. 4). The size of the ROIs was 2 mm in length and 2 mm in width. The metal artifact index proposed by Yasaka et al.[9] was calculated on the buccal and lingual sides using the following formula:

Metal artifact index = $|(\text{SDs with dental implants})^2 - (\text{SDs in control})^2|^{1/2}$

Also, changing rates of CT values on the mesial and distal sides were calculated in the same way as outlined in the above-mentioned method.

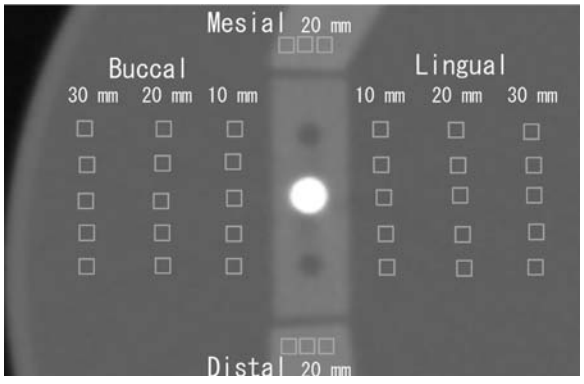

Fig. 4. Setting of ROIs in regions far from titanium dental implants

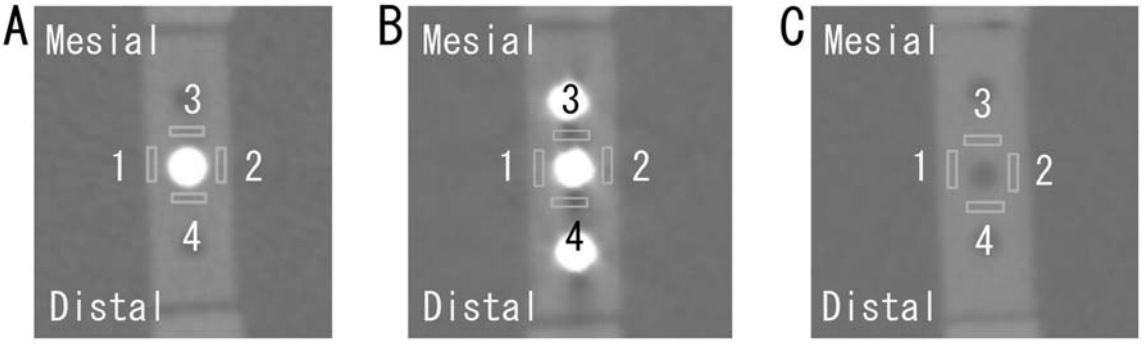

Fig. 3. Setting of ROIs surrounding titanium dental implants
A: One dental implant
B: Three dental implants
C: Control
1: Buccal side, 2: Lingual side, 3: Mesial side, 4: Distal side

Results

CT values surrounding dental implants

The mean CT values and standard deviations (SDs) with each image are shown in Tables 1 and 2. CT values on the mesial and distal sides with three dental implants were below zero in almost all images with all image reconstruction functions. Standard deviations in the control were smaller than those with one or three dental implants.

Changing rates of CT values in each image are shown in Fig. 5. Changing rates of CT values on the buccal, lingual, and mesial sides with one dental implant were relatively small in images with a soft tissue image reconstruction function. Changing rates of CT values on the distal side with one dental implant were more than 10% in all images. Changing rates of CT values with three dental implants were larger than those with one dental implant using a soft tissue image reconstruction function, especially on the mesial and distal sides. Changing rates of CT values on all sides with one dental implant and on the buccal and lingual sides with three dental implants using a soft tissue reconstruction function with SEMAR were larger than those using a soft tissue image reconstruction function without SEMAR. Changing rates of CT values in 120-kV images were similar to those in 135-kV images.

CT values in regions far from dental implants

The mean CT values and SDs with each image are shown in Tables 3, 4, and 5. Also, metal artifact indexes with each image on the buccal and lingual sides are shown in Fig. 6 and changing rates of CT values with each image on the mesial and distal sides are shown in Fig. 7. Metal artifact indexes with three dental implants at 10 mm on the buccal and lingual sides were larger than those with one dental implant in all images. Metal artifact indexes on the lingual side with three dental implants in images using a soft tissue reconstruction function with SEMAR were smaller than those using a soft tissue reconstruction function in 120-kV images. Changing rates of CT values on the mesial and distal sides with one or three dental implants were comparatively large in images with the bone image reconstruction function. Changing rates on the mesial and distal sides with three dental implants in images using a soft tissue reconstruction function with SEMAR were smaller than those using a soft tissue reconstruction function in 120-kV and 135-kV images.

Table 1. Mean CT values and standard deviations surrounding Ti dental implants

Dental implants	Tube voltages (kV)	Image reconstruction factors	Sides Buccal	Lingual	Mesial	Distal
One	120	bone	394.1 (45.0)	309.2 (25.6)	264.3 (31.1)	189.5 (66.1)
	120	soft	332.3 (31.4)	320.6 (22.0)	344.2 (23.8)	258.6 (8.2)
	120	soft+SEMAR	382.1 (28.1)	397.1 (17.6)	175.6 (23.9)	166.6 (12.6)
	135	bone	374.5 (51.1)	307.5 (36.9)	223.7 (52.1)	207.6 (48.6)
	135	soft	307.0 (8.5)	278.7 (9.4)	285.7 (16.6)	234.7 (9.7)
	135	soft+SEMAR	383.1 (25.5)	368.7 (12.3)	142.8 (20.8)	131.4 (21.5)
Three	120	bone	412.1 (95.0)	354.4 (69.0)	−509.6 (92.9)	−273.7 (76.6)
	120	soft	389.4 (38.6)	379.7 (12.0)	−150.9 (31.6)	−118.7 (6.5)
	120	soft+SEMAR	583.4 (21.0)	606.1 (14.3)	−36.7 (24.2)	8.1 (18.2)
	135	bone	456.7 (100.2)	424.1 (18.6)	−571.3 (56.6)	−331.7 (79.9)
	135	soft	382.4 (40.1)	337.5 (15.4)	−164.0 (25.2)	−117.4 (30.8)
	135	soft+SEMAR	537.7 (23.6)	567.6 (14.2)	−98.3 (13.1)	−21.1 (11.4)

Units: HU

Table 2. Mean control CT values and standard deviations surrounding Ti dental implants

Tube voltages (kV)	Image reconstruction factors	Sides Buccal	Lingual	Mesial	Distal
120	bone	344.6 (9.4)	334.9 (3.5)	344.7 (4.7)	330.2 (3.9)
120	soft	312.1 (2.5)	302.5 (5.0)	319.6 (1.5)	321.3 (1.5)
120	soft+SEMAR	308.1 (5.3)	299.7 (4.9)	318.9 (2.5)	321.8 (1.7)
135	bone	332.5 (8.9)	323.2 (7.6)	320.3 (4.3)	321.1 (6.2)
135	soft	285.2 (4.7)	278.1 (5.5)	291.5 (2.8)	294.6 (2.6)
135	soft+SEMAR	284.4 (5.5)	279.0 (6.2)	292.4 (1.8)	295.6 (2.1)

Units: HU

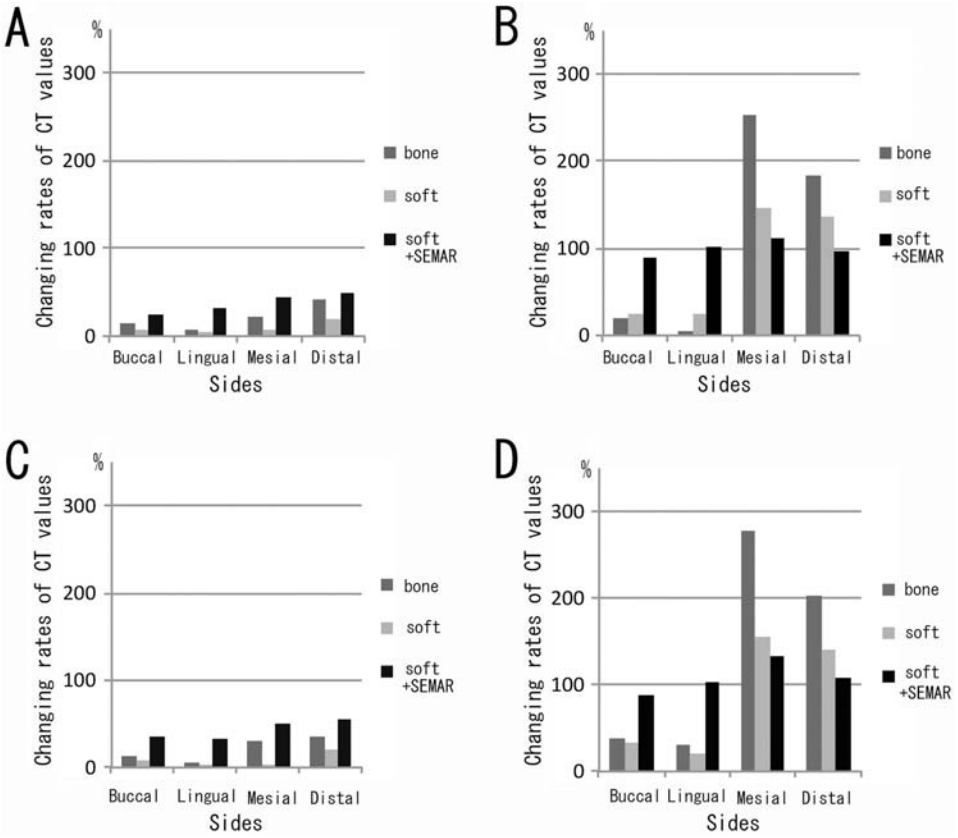

Fig. 5. Changing rates of CT values surrounding titanium dental implants
A: 120-kV images with one dental implant, B: 120-kV images with three dental implants
C: 135-kV images with one dental implant, D: 135-kV images with three dental implants

Table 3. Mean CT values and standard deviations on buccal and lingual sides far from Ti dental implants

Dental implants	Tube voltages (kV)	Image reconstruction factors	Locations Buccal 10 mm	20 mm	30 mm	Lingual 10 mm	20 mm	30 mm
One	120	bone	13.9 (6.0)	7.0 (6.9)	3.9 (4.8)	11.3 (7.7)	5.2 (5.8)	5.2 (5.9)
	120	soft	9.7 (6.7)	7.8 (4.5)	7.1 (3.0)	6.3 (4.6)	3.8 (3.6)	3.2 (3.1)
	120	soft+SEMAR	16.3 (7.6)	8.4 (3.9)	7.5 (2.9)	13.3 (6.3)	5.6 (3.5)	3.8 (3.1)
	135	bone	6.6 (4.0)	5.0 (6.2)	1.0 (4.9)	8.8 (8.2)	6.4 (6.1)	4.2 (5.2)
	135	soft	6.9 (3.3)	4.7 (3.9)	4.4 (3.0)	5.5 (4.9)	4.3 (3.9)	1.3 (2.9)
	135	soft+SEMAR	14.0 (6.5)	7.1 (4.0)	5.4 (2.0)	10.4 (7.1)	5.0 (3.4)	1.5 (3.3)
Three	120	bone	17.7 (13.4)	7.1 (6.9)	4.0 (7.2)	19.1 (18.2)	7.1 (7.4)	4.1 (5.8)
	120	soft	12.8 (14.8)	8.3 (3.8)	5.3 (4.3)	13.1 (13.9)	4.7 (3.5)	2.4 (3.6)
	120	soft+SEMAR	36.8 (11.4)	16.1 (7.7)	12.1 (3.3)	31.6 (8.6)	13.7 (2.2)	9.8 (3.2)
	135	bone	19.0 (11.3)	5.0 (5.8)	2.4 (5.5)	16.4 (12.5)	8.3 (4.9)	4.3 (5.4)
	135	soft	15.5 (6.0)	4.5 (3.6)	3.9 (2.7)	9.8 (10.4)	3.5 (3.2)	2.4 (3.9)
	135	soft+SEMAR	32.3 (10.9)	12.2 (6.2)	8.4 (3.2)	28.2 (6.2)	12.1 (2.9)	7.0 (3.7)

Units: HU

Table 4. Mean control CT values and standard deviations on buccal and lingual sides far from Ti dental implants

Tube voltages (kV)	Image reconstruction factors	Locations Buccal 10 mm	20 mm	30 mm	Lingual 10 mm	20 mm	30 mm
120	bone	6.4 (6.4)	3.9 (5.3)	3.9 (5.0)	6.1 (4.4)	7.0 (5.4)	3.5 (5.2)
120	soft	6.6 (3.2)	5.4 (2.9)	5.2 (1.7)	2.7 (3.0)	3.8 (2.9)	1.5 (2.9)
120	soft+SEMAR	6.2 (2.4)	5.3 (3.1)	5.1 (1.7)	3.1 (2.3)	3.3 (2.8)	1.5 (3.0)
135	bone	4.6 (2.9)	2.4 (5.8)	0.9 (3.2)	4.0 (5.7)	7.2 (5.9)	5.1 (4.6)
135	soft	4.4 (1.8)	3.6 (3.0)	2.5 (2.2)	2.4 (2.6)	2.7 (3.3)	0.9 (3.2)
135	soft+SEMAR	4.5 (2.0)	3.9 (2.7)	2.7 (1.6)	3.3 (2.5)	2.9 (2.5)	1.3 (3.8)

Units: HU

Table 5. Mean CT values and standard deviations on mesial and distal sides far from Ti dental implants

Tube voltages (kV)	Image reconstruction factors	one dental implant		three dental implants		Control	
		Mesial 20 mm	Distal 20 mm	Mesial 20 mm	Distal 20 mm	Mesial 20 mm	Distal 20 mm
120	bone	422.1 (7.1)	426.4 (6.1)	341.8 (8.8)	336.0 (8.9)	449.4 (7.0)	434.9 (3.8)
120	soft	402.4 (3.1)	407.4 (2.1)	334.0 (3.4)	329.3 (7.1)	418.2 (1.5)	411.2 (1.4)
120	soft+SEMAR	441.9 (10.7)	455.5 (7.2)	459.8 (13.2)	467.8 (49.9)	416.9 (2.4)	411.7 (1.3)
135	bone	393.9 (6.0)	395.8 (5.1)	331.6 (7.3)	330.5 (8.4)	428.7 (7.9)	404.9 (7.9)
135	soft	356.2 (2.3)	358.0 (2.5)	310.0 (3.7)	310.3 (6.9)	373.0 (3.3)	364.4 (3.7)
135	soft+SEMAR	401.6 (10.8)	404.8 (13.3)	411.0 (11.2)	393.4 (63.1)	375.3 (2.5)	364.6 (3.7)

Units: HU

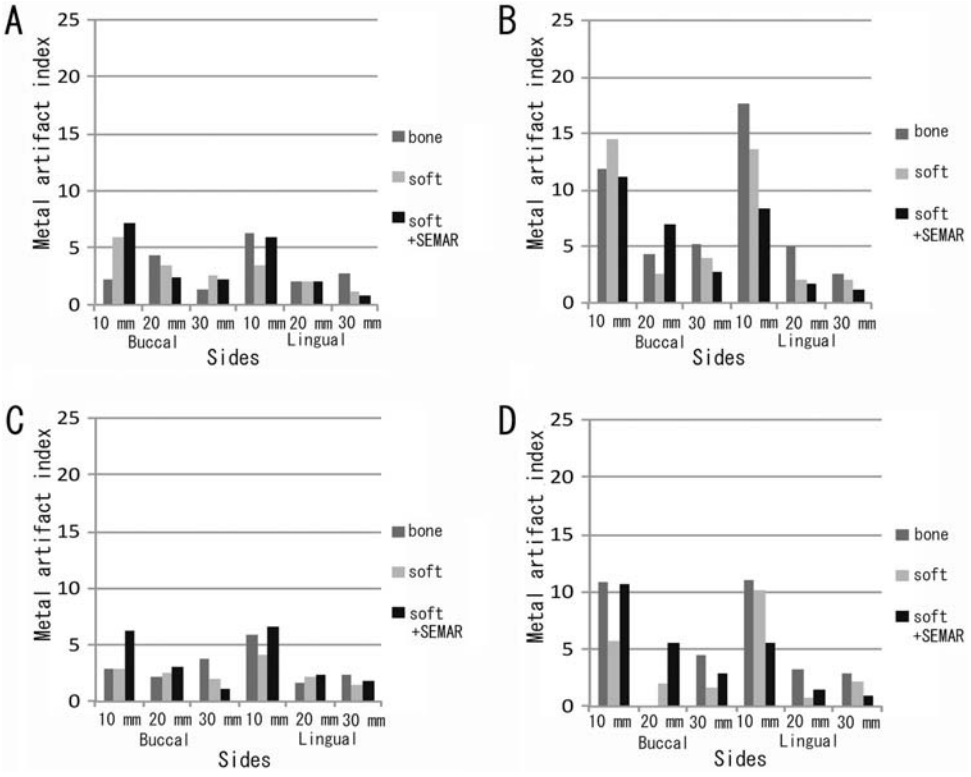

Fig. 6. Metal artifact index on buccal and lingual sides far from titanium dental implants
A: 120-kV images with one dental implant, B: 120-kV images with three dental implants
C: 135-kV images with one dental implant, D: 135-kV images with three dental implants

Discussion

Postoperative diagnostic imaging of dental implant treatment is important for an accurate prognosis over long-term follow-up[2-4]. Therefore, in the present study, metal artifacts generated by Ti dental implants in multi-detector CT were experimentally assessed using mandibular phantoms.

Various phantoms were used in previous experimental studies to assess metal artifacts generated by dental implants[12,15-17]. In the present study, the mandibular phantom was made using bone blocks and radiopaque acrylic resin. Dental implants - either one or three - were implanted into the bone blocks. The bone blocks had equivalent CT values to cancellous bone and were homogeneous.

In many previous studies, metal artifacts generated by dental alloys were assessed using qualitative image analysis by readers, as well as quantitative image analysis in regions far from dental alloys. Moreover, in quantitative analysis, CT values and their SDs were used. Yasaka et al.[9] and Kubo et al.[13] proposed a metal artifact index calculated from SDs in tongue and nuchal muscles. Moreover, Bongers et al.[8] applied a Fourier-based method in hip prosthesis and dental implants. In the

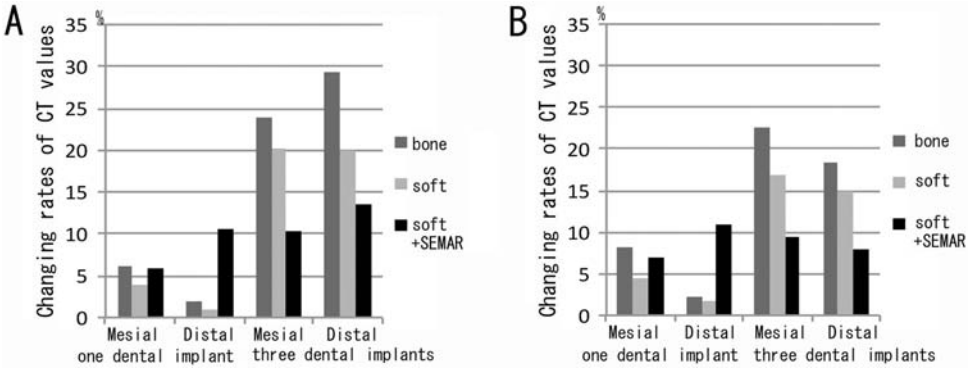

Fig. 7. Changing rates of CT values on mesial and distal sides far from titanium dental implants
A: 120-kV images, B: 135-kV images

present study, CT values were measured on the buccal, lingual, mesial, and distal sides surrounding dental implants, and in regions far from them to evaluate metal artifacts generated by Ti dental implants, and the fluctuation of CT values was considered an influence of such metal artifacts. CT values obtained from multi-detector CT are absolute values[18,19].

As the results of CT values surrounding dental implants, changing rates of CT values with one dental implant on the buccal, lingual, and mesial sides were relatively small in 120- and 135-kV images with a soft tissue image reconstruction function. However, CT values with three dental implants on the mesial and distal sides were below zero in almost all images with all image reconstruction functions, and changing rates of CT values with three dental implants were larger than those with one dental implant. CT values on the buccal and lingual sides with one or three dental implants were higher in comparison with the control in images with a soft tissue image reconstruction function. Moreover, CT values on the mesial and distal sides with three dental implants were smaller in comparison with the control in images with soft tissue and bone image reconstruction functions. Differences in CT values surrounding dental implants might be influenced by beam-hardening effects. Beam-hardening effects are related to dental implants and the mandibular form, and are complex. If increases in CT values caused by metal artifacts are clinically observed, like on the buccal and lingual sides in this study, any decreases in CT values caused by bone resorption in peri-implantitis might be balanced out by fluctuations in metal artifacts. Moreover, if decreases in CT values due to metal artifacts are clinically observed, like on the mesial and distal sides in this study, the condition might be inaccurately diagnosed as peri-implantitis. Thus, it may be difficult for peri-implantitis to be accurately diagnosed using multi-detector CT. Changing rates of CT values with one dental implant on all sides and with three dental implants on the buccal and lingual sides using a soft tissue reconstruction function with SEMAR were larger than those using a soft tissue image reconstruction function without SEMAR in 120- and 135-kV images. The effect of metal artifact reduction using the SEMAR algorithm was not observed when evaluating CT values surrounding dental implants.

Yasaka et al.[9] and Kubo et al.[13] calculated a metal artifact index using standard deviations in tongue and nuchal muscles to evaluate metal artifacts in the tongue far from dental alloys made of gold, silver, palladium, etc. Yasaka et al.[9] reported that the SEMAR algorithm could provide images with reduced metal artifacts. In the present study, the formula for calculation of the metal artifact index was modified. The metal artifact index on the lingual side with three dental implants in images using a soft tissue reconstruction function with SEMAR were smaller than those using a soft tissue reconstruction function in 120-kV images, and a similar tendency was noted. The range of the metal artifact index was from 0.0 to 17.7 in the present study. Yasaka et al.[9] reported that the metal artifact range was from 57.8 to 161.1 with a mean of 88.4. The values were larger than those in the present study. The atomic number of dental alloys was larger than that of dental implants made of Ti, and metal artifacts generated by dental alloys were marked.

In the future, improvement of metal artifact reduction

algorithms will be necessary for diagnostic imaging in the oral and maxillofacial region during Ti dental implant treatment.

Conclusion

In the present study, metal artifacts generated by Ti dental implants were experimentally assessed using mandibular phantoms. No effect of metal artifact reduction using the SEMAR algorithm was observed surrounding Ti dental implants. The effect of metal artifact reduction using the SEMAR algorithm was limited in regions far from the implants.

Acknowledgement

We would like to thank Mr. Kenichi Gotoh, Mr. Ryo Matsumoto, and Mr. Tsutomu Kuwada of the Division of Radiology, Dental Hospital, at the Aichi Gakuin University for their corporation in performing multi-detector CT.

The authors have no conflicts of interest to declare.

References

1) Misch CE: Contemporary Implant Dentistry. 3rd ed. Mosby (St. Louise), 1-25, 2008.
2) Naitoh M, Dula K, Ito Y, Toyoda T, Kurita K, Ariji E: Postoperative tomographic assessment of veneer bone grafting with implant placement in the maxillary anterior region. Implant Dent, **14**(3): 301-307, 2005.
3) Naitoh M, Nabeshima H, Hayashi H, Nakayama T, Kurita K, Ariji E: Postoperative assessment of incisor dental implants using cone-beam computed tomography. J Oral Implantol, **36**(5): 377-384, 2010.
4) Naitoh M, Hayashi H, Tsukamoto N, Ariji E: Labial bone assessment surrounding dental implant using cone-beam computed tomography: an *in vitro* study. Clin Oral Impl Res, **23**(8): 970-974, 2012.
5) Naitoh M, Katsumata A, Nohara E, Ohsaki C, Ariji E: Measurement accuracy of reconstructed 2-D images obtained by multi-slice helical computed tomography. Clin Oral Impl Res, **15**(5): 570-574, 2004.
6) Naitoh M, Katsumata A, Mitsuya S, Kamemoto H, Ariji E: Measurement of mandibles with microfocus x-ray computerized tomography and compact computerized tomography for dental use. Int J Oral Maxillofac Implants, **19**(2): 239-246, 2004.
7) Hayashi T, Committee on Clinical Practice Guidelines, Japanese Society for Oral and Maxillofacial Radiology: Guideline of Diagnostic Imaging for a Dental Implamt Treatment in Japan. Minds, 2008. http://www.minds.jcqhc.or.jp/n/med/4/med0060/G0000166/0001 (accessed: Aug 16, 2022)
8) Bongers MN, Schabel C, Thomas C, Raupach R, Notohamiprodjo M, Nikolaou K, Bamberg F: Comparison and combination of dual-energy- and interactive- based metal artifact reduction on hip prosthesis and dental implants. PloS One, **10**(11): e0143584, 2015.
9) Yasaka K, Kamiya K, Irie R, Maeda E, Sato J, Ohtomo K: Metal artifact reduction for patients with metallic dental fillings in helical neck computed tomography: comparison of adaptive iterative dose reduction 3D (AIDR 3D), forward-projected model-based interactive reconstruction solution (FIRST) and AIDR 3D with single-energy metal artifact reduction (SEMAR). Dentomaxillofac Radiol, **45**(7): 20160114, 2016.
10) Kellock TT, Nicolaou S, Kim SS, Al-Busaidi S, Louis LJ, O'Connell TN, Ouellette HA, McLaughlin PD: Detection of bone marrow edema in nondisplaced hip fractures: utility of a virtual noncalcium dual-energy CT application. Radiol, **284**(3): 798-805, 2017.
11) Garner HW, Paturzo MM, Gaudier G, Pickhardt PJ, Wessell DE: Variation in attenuation in L1 trabecular bone at different tube voltages: Caution is warranted when screening for osteoporosis with the use of opportunistic CT. AJR Am J Roentgenol, **208**(1): 165-170, 2017.
12) Long Z, Bruesewitz MR, DeLone DR, Morris JM, Amrami KK, Adkins MC, Glazebrook KN, Kofler JM, Leng S, McCollough CH, Fletcher JG, Halaweish AF, Yu L: Evaluation of projection- and dual-energy-based methods for metal artifact reduction in CT using a phantom study. J Appl Clin Med Phys, **19**(4): 252-260, 2018.
13) Kubo Y, Ito K, Sone M, Nagasawa H, Onishi Y, Umakoshi N, Hasegawa T, Akimoto T, Kusumoto M: Diagnostic value of model-based iterative reconstruction combined with a metal artifact

reduction algorithm during CT of the oral cavity. AJNR Am J Neuroradiol, **41**(11): 2132-2138, 2020.

14) Schmidt AMA, Grunz J-P, Petritsch B, Gruschwitz P, Knar J, Huflage H, Bley TA, Kosmala A: Combination of iterative metal artifact reduction and virtual monoenergetic reconstruction using split-filter dual-energy CT in patients with dental artifact on head and neck CT. AJR Am J Roentgenol, **218**(4): 716-722, 2022.

15) Pauwels R, Stamatakis H, bosmans H, Bogaerts R, Jacobs R, Horner K, Tsiklakis K, SEDENTEXCTCT Project Consortium: Quantification of metal artifacts on cone beam computed tomography images. Clin Oral Impl Res, **24**(suppl A100): 94-99, 2013.

16) Naitoh M, Hikita R, Watanabe H, Miyamae S, Saburi K, Gotoh K, Ariji E: Assessment of metal artifacts surrounding dental implants using cone-beam computed tomography: An *in vitro* study. Aichi Gakuin Dent Sci, **29**(1): 19-25, 2016.

17) Naitoh M, Watanabe H, Hikita R, Gotoh K, Miyamae S, Ariji E: Assessment of dental implant interface in cone-beam computed tomography: an *in vitro* study. Aichi Gakuin Dent Sci, **31**(1): 23-30, 2018.

18) Naitoh M, Kurosu Y, Inagaki K, Katsumata A, Noguchi T, Ariji E: Assessment of mandibular buccal and lingual cortical bones in postmenopausal women. Oral Surg Oral Med Oral Pathol Oral Radiol Endod, **104**(4): 545-550, 2007.

19) Misch CE: Contemporary Implant Dentistry, 3rd ed. Mosby (St. Louis), 38-67, 2008.